Supporting Information

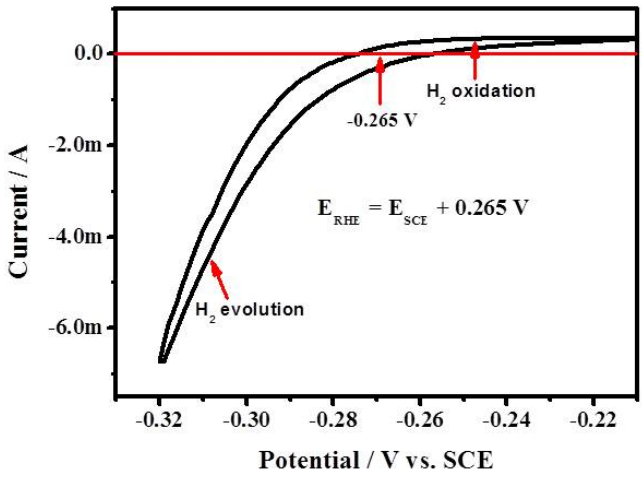

Figure S1. Cyclic voltammogram depicting the calibration of saturated calomel electrode with respect to RHE. Scan rate used is 1 mV s^{-1}, in presence of H_2 saturated solution in 0.5 mol L^{-1} H_2SO_4.

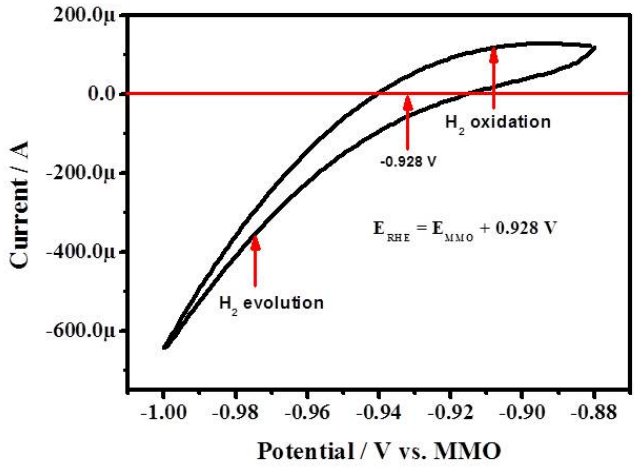

Figure S2. Cyclic voltammogram depicting the calibration of MMO with respect to RHE. Scan rate used is 1 mV s^{-1} in presence of H_2 saturated solution in 0.1 mol L^{-1} KOH.

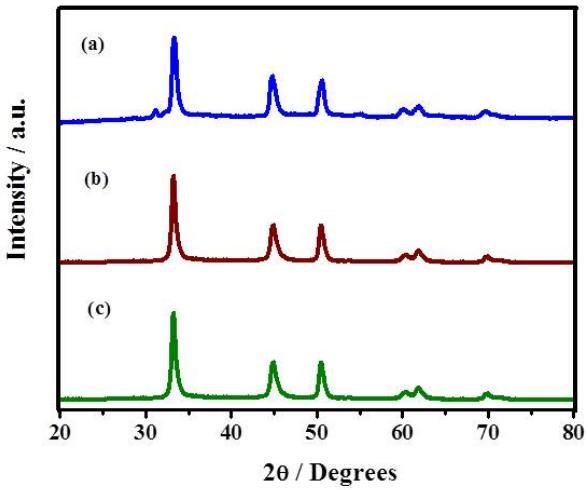

Figure S3. Powder X-ray diffraction patterns of NiSe wires prepared at different of reaction times at a temperature of 180°C (a) 3 h, (b) 5 h and (c) 8 h. The concentration of Ni and Se source used is 1:3 mole ratios of $NiCl_2.6H_2O$ and selenourea.

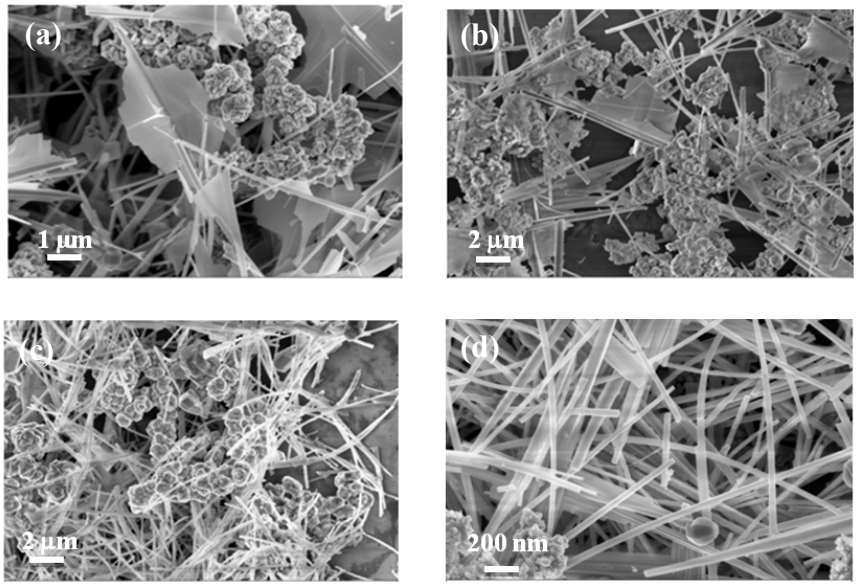

Figure S4. Scanning electron microscopy images of NiSe wires prepared at different reaction times of (a) 1 h, (b) 3 h, (c) 5 h and (d) 8 h. 1:3 mole ratio of $NiCl_2.6H_2O$ and selenourea is used at a temperature of 180°C.

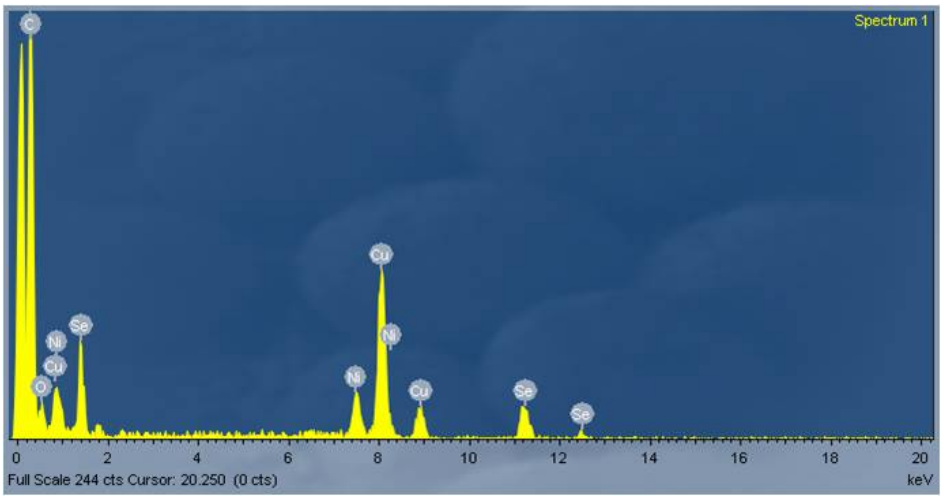

Figure S5. EDAX pattern of NiSe wires.

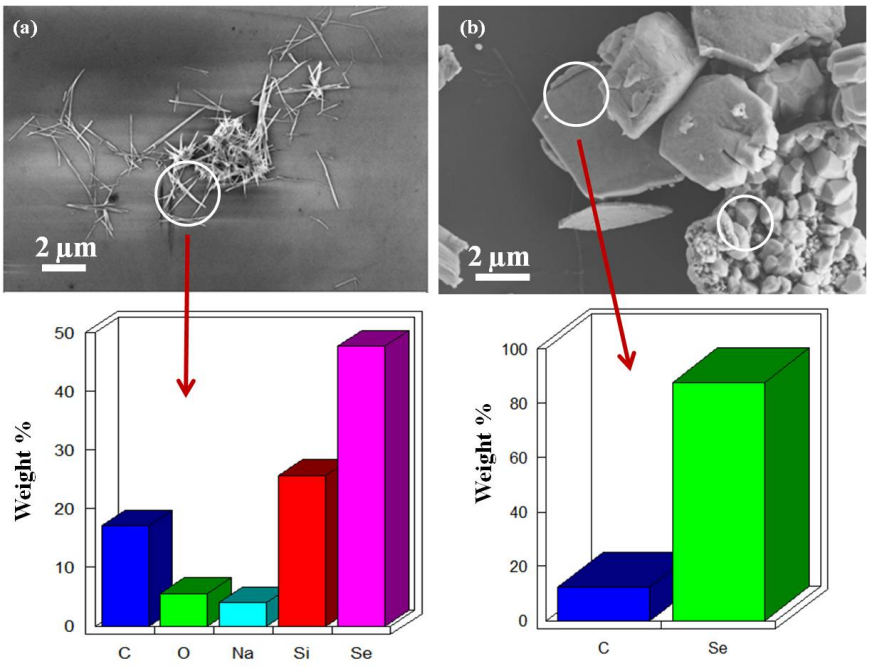

Figure S6. SEM images of (a) selenium wires and (b) selenium hexagons formed selenourea and KSeCN precursors in the absence of nickel salt. Temperature used is 180°C and time of reaction is maintained for 8 h.

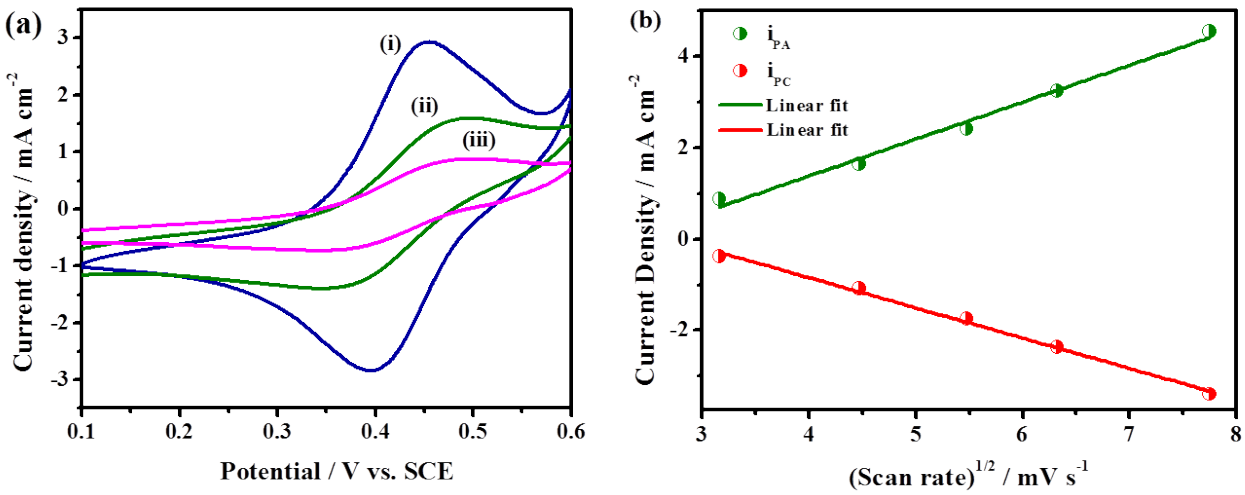

Figure S7. Cyclic voltammograms of 10 mmol L^{-1} $K_4[Fe(CN)_6]$ in 0.1 mol L^{-1} KCl on (a) NiSe nanowires (i), spheres (ii) and hexagons (iii) on a modified glassy carbon electrode at a scan rate on 50 mV s^{-1} and (b) linear relation between cathodic and anodic current density vs. $(\text{scan rate})^{1/2}$ for NiSe nanowires.

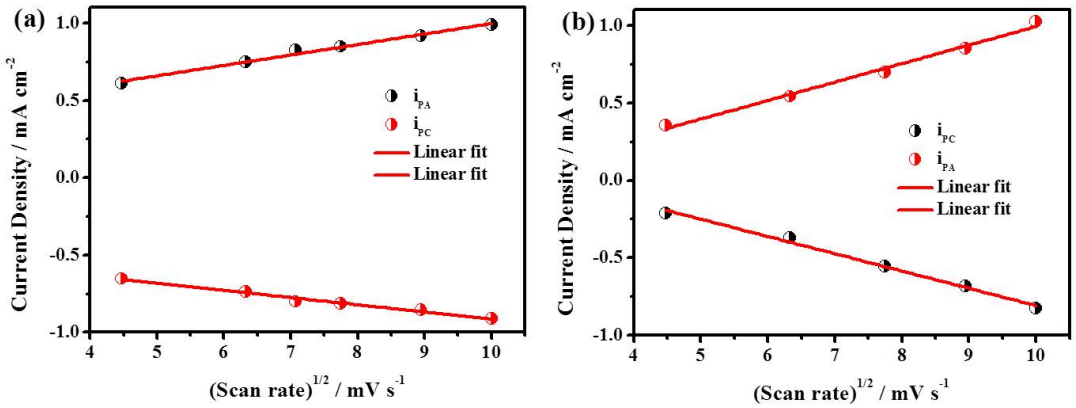

Figure S8. Linear relation between cathodic and anodic current density vs. $(\text{scan rate})^{1/2}$ for (a) NiSe spheres and (b) hexagons.

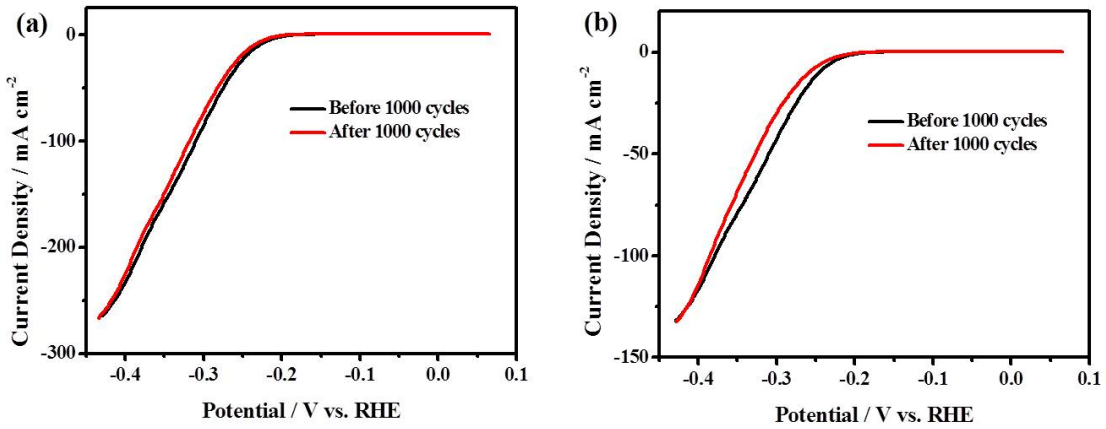

Figure S9. Linear sweep voltammograms for the NiSe (a) spheres and (b) hexagons before and after 1000 cycles.

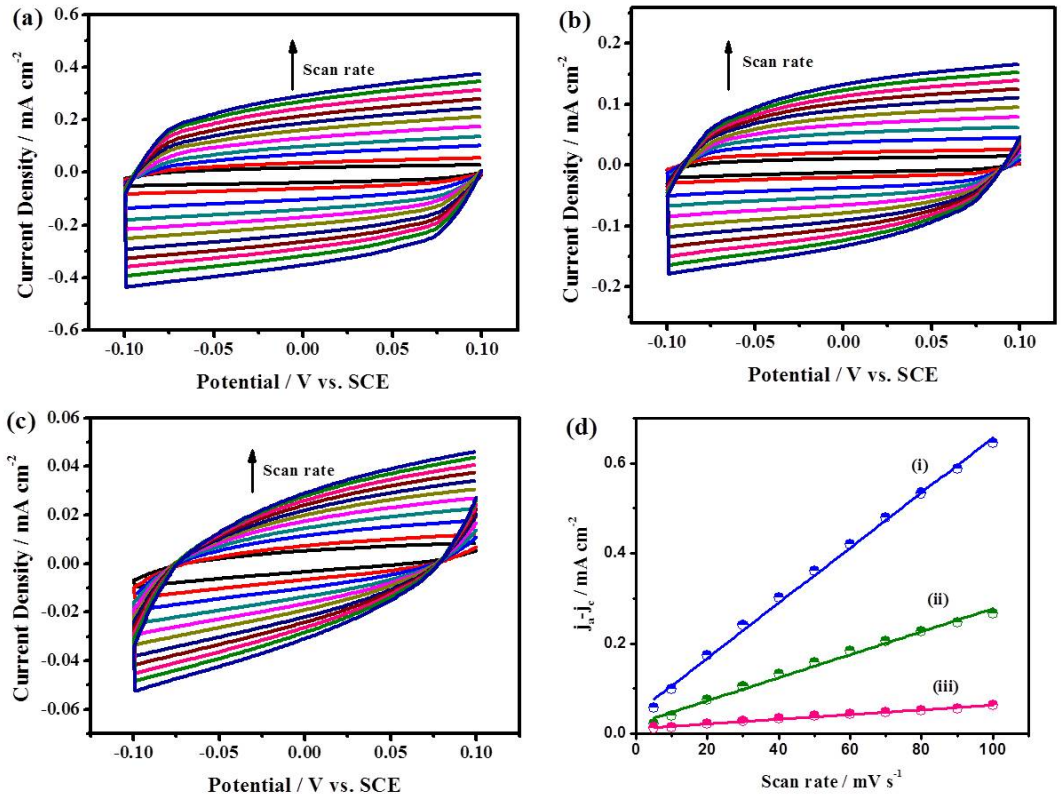

Figure 10. Cyclic voltammograms of (a) NiSe wires, (b) NiSe spheres and (c) NiSe hexagons in the non-faradic region in 0.5 mol L^{-1} H_2SO_4 electrolyte. (d) Scan rate dependence of voltamograms of three morphologies (i) wires, (ii) spheres and (iii) hexagons at 0 V vs. SCE.

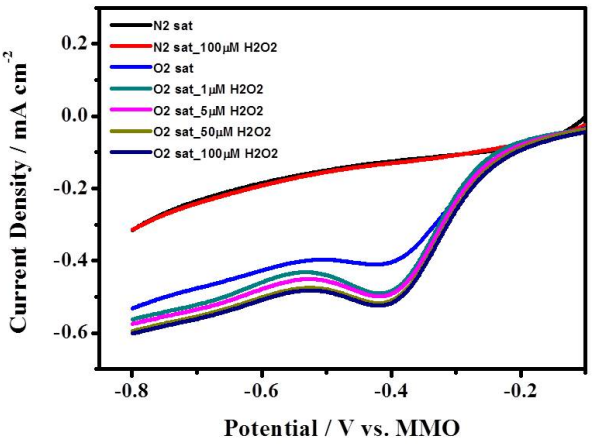

Figure S11. Effect of addition of H_2O_2 of different concentrations (1 μmol L^{-1} to 100 μmol L^{-1}) in presence of O_2 saturated 0.1 mol L^{-1} KOH solution on NiSe wire as active catalyst. Control experiments in the absence of oxygen as well as only in the presence of O_2 are also given.

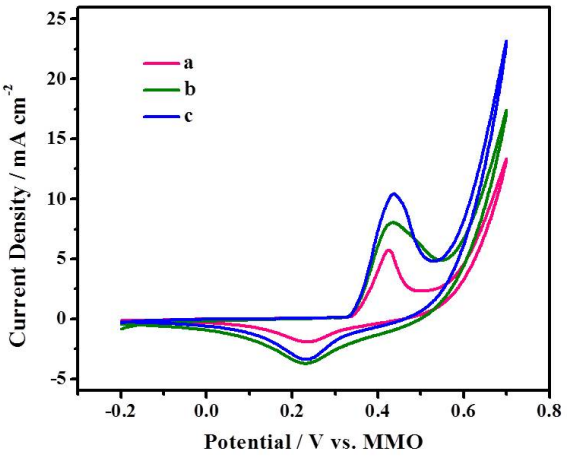

Figure S12. Cyclic voltammograms on NiSe nanowires (c), spheres (b) and hexagons (a) in 0.5 mol L^{-1} NaOH containing of 0.5 mmol L^{-1} glucose at a scan rate of 20 mV s^{-1}.

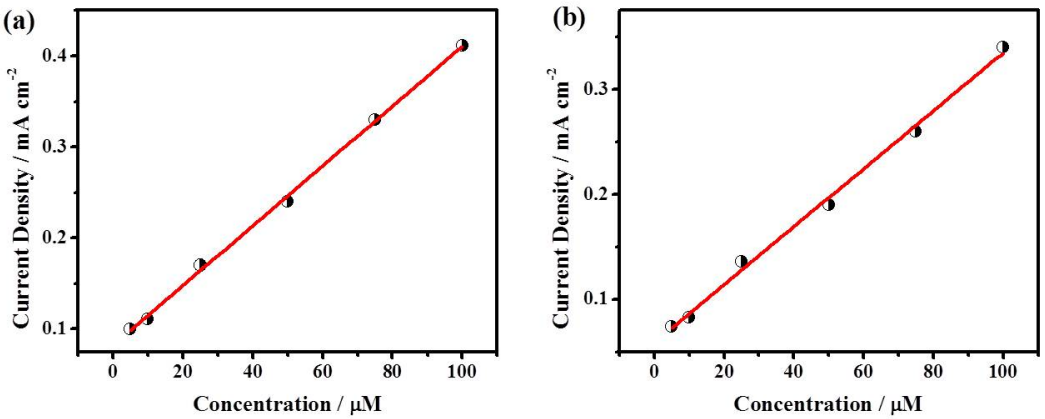

Figure S13. Calibration plots obtained on NiSe (a) spheres and (b) hexagons for glucose oxidation.